



**HAL**  
open science

## Evolution of Corrections Processing for MC/MF Ground Based Augmentations System (GBAS)

Carl Milner, Alizé Guilbert, Christophe Macabiau

► **To cite this version:**

Carl Milner, Alizé Guilbert, Christophe Macabiau. Evolution of Corrections Processing for MC/MF Ground Based Augmentations System (GBAS). International Technical Meeting 2015, Institute of Navigation, Jan 2015, Dana Point, United States. hal-01147281

**HAL Id: hal-01147281**

**<https://enac.hal.science/hal-01147281>**

Submitted on 30 Apr 2015

**HAL** is a multi-disciplinary open access archive for the deposit and dissemination of scientific research documents, whether they are published or not. The documents may come from teaching and research institutions in France or abroad, or from public or private research centers.

L'archive ouverte pluridisciplinaire **HAL**, est destinée au dépôt et à la diffusion de documents scientifiques de niveau recherche, publiés ou non, émanant des établissements d'enseignement et de recherche français ou étrangers, des laboratoires publics ou privés.

# Evolution of Corrections Processing for MC/MF Ground Based Augmentations System (GBAS)

Dr. Carl Milner, Alizé Guilbert & Dr. Christophe Macabiau, *Ecole Nationale de l'Aviation Civile, Toulouse France*

## BIOGRAPHIES

**Dr. Carl MILNER** is an Assistant Professor within the Telecom Lab at the Ecole Nationale Aviation Civile (ENAC) in Toulouse, France. He has a Master's degree in Mathematics from the University of Warwick, a PhD in Geomatics from Imperial College London and has completed the graduate trainee Programme at the European Space Agency. His research interests include GNSS augmentation systems, integrity monitoring, air navigation and applied mathematics.

**Alizé GUILBERT** is a French PhD student. She received in 2012 an Engineer Diploma from the ENAC with a specialization in Aeronautical Telecommunications. She is currently doing a PhD in the SIGNAV laboratory at the ENAC for the SESAR (Single European Sky Air traffic management Research) project (WP15.3.7) since April 2013. Her subject is *the Development of Processing Models for Multi-Constellation/Multi-frequency (MC/MF) GBAS*.

**Dr. Christophe MACABIAU** graduated as an electronics engineer in 1992 from the ENAC. Since 1994, he has been working on the application of satellite navigation techniques to civil aviation. He received his PhD in 1997 and has been in charge of the signal processing lab of ENAC since 2000.

## ABSTRACT

The Ground Based Augmentation System (GBAS) is currently standardized at the International Civil Aviation Organization (ICAO) level to provide precision approach navigation services up to Category I using the GPS or GLONASS constellations [1]. Current investigations into the use of GBAS for a Category II/III service type known as GAST D are ongoing [2]. However, some gaps in performance have been identified and open issues remain [3]. Multi-frequency and multi-constellation solutions are being explored within the European SESAR program (WP 15.3.7) to address these issues. The addition of a secondary constellation provides many advantages such as better geometry, robustness against signal outages, relaxing of demanding constraints. Furthermore, new signals offer the potential to combine measurements on multiple frequencies to mitigate the effects of the ionosphere,

including during disturbances and helps the stringent continuity and availability requirements to be met [4].

However, whilst the advantages of using many more signals is clear, there exists a major constraint with respect to the available space for message transmission from the GBAS VHF Data Broadcast (VDB) unit [5]. Currently, corrections and their integrity are provided in combined messages broadcast every half second (2Hz). However, extending this approach to multiple correction types, based on the different signals and observables for two or more constellations will not be possible. Furthermore, if the need arises to include future signals from the modernized constellations or expand further than two constellations then no additional transmission space would be available. It is for these reasons that the authors have investigated the possibility of providing corrections at a lower rate than the current 2Hz, with a separate message type dedicated to providing the integrity status of each correction in a manner akin to the Satellite Based Augmentation System (SBAS) [6].

In order to justify this approach and to select the ideal correction message rate, a number of items must be addressed.

## INTRODUCTION

The Ground Based Augmentation System (GBAS) is currently standardized at the International Civil Aviation Organization (ICAO) level to provide precision approach navigation services up to Category I using the GPS or GLONASS constellations [1]. Current investigations into the use of GBAS for a Category II/III service type known as GAST D are ongoing [2]. However, some gaps in performance have been identified and open issues remain [3]. Multi-frequency and multi-constellation solutions are being explored within the European SESAR program (WP 15.3.7) to address these issues. The addition of a secondary constellation provides better geometry which could enable lower performing aircraft, with higher Flight Technical Error (FTE) to gain certification for these most stringent operations. Furthermore, for all aircraft operating in challenging environments such as regions of ionospheric scintillation, the better geometry provides robustness against signal outages and helps the stringent continuity and availability requirements to be met [4].

In addition, new signals offer the potential to combine measurements on multiple frequencies to mitigate the effects of the ionosphere, including during disturbances which result in gradients and plasma bubbles [7]. The current single-frequency GAST D requirements include demanding constraints (siting, threat model validation) whose principal role is to protect the system against such ionospheric threats. Even in the presence of an ionospheric gradient, precision approach services to Category II/III could be maintained if multiple correction types are utilized. Furthermore, the additional signal redundancy would provide better robustness to other effects such as scintillation and interference.

However, whilst the advantages of using many more signals is clear, there exists a major constraint with respect to the available space for message transmission from the GBAS VHF Data Broadcast (VDB) unit [5]. Currently, corrections and their integrity are provided in combined messages broadcast every half second (2Hz). However, extending this approach to multiple correction types, based on the different signals and observables for two or more constellations will not be possible. Furthermore, if the need arises to include future signals from the modernized constellations or expand further than two constellations then no additional transmission space would be available. It is for these reasons that the authors have investigated the possibility of providing corrections at a lower rate than the current 2Hz, with a separate message type dedicated to providing the integrity status of each correction in a manner akin to the Satellite Based Augmentation System (SBAS) [6].

In order to justify this approach and to select the ideal correction message rate, a number of items must be addressed.

This paper first presents GBAS processing architecture with one of the proposed MF processing models in the form of the ionosphere-free smoothing. Then, Single frequency error models are then presented which critically contribute to the range-rate corrections. The properties of the range-rate corrections are key to understanding how an increase in the correction update period will impact the total performance of the system. The total error budget is then derived which allows a quantification of the degradation in the corrections as a function of the message update rate. Theoretical curves are then presented for the current MT1 and MT11 corrections based on 100s and 30s smoothing constants respectively. Furthermore, a real data analysis performed with single frequency GPS L1 data to validate models and to compare results with the theoretical curves obtained is presented. Indeed, several simulations for analyzing the influence of an increased update rate of PRC and RRC were processed by comparing extrapolation of PRC for 1.5s with extrapolation of PRC for other extended times.

The paper concludes that an update period of 1.5-2.5s is the preferred choice for the next generation MC/MF GBAS, known as GAST F. A proposed VDB transmission

structure is included to determine the number of corrections, the product of the number of ranging sources and number of correction types, which may be broadcast whilst maintaining integrity under the proposed GAST F design.

## GAST D PROCESSING ARCHITECTURE

The GBAS ground subsystem processing (described in Figure 1) must transmit through the VHF Data Broadcast (VDB) unit several message types which include the correction parameters for each satellite (according to MOPS [8]): Pseudo Range Correction (PRC) and Range Rate Correction (RRC).

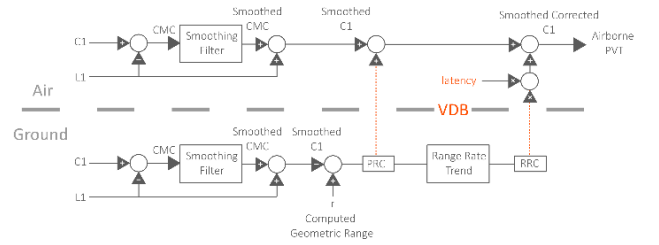


Figure 1- GBAS Processing Architecture

For GAST D both Message Type 1 (MT1) and Message Type 11 (MT11) are used to provide corrections with both 100s and 30s smoothing respectively [8] [9] [10]. The longer smoothing constant corrections in MT1 mitigate to a greater extent the high frequency components of multipath and noise but suffer from greater ionospheric divergence than the 30s corrections contained in MT11. The measurement model used in this paper is as follows [5] [11]:

$$\rho_1^G = r^G + dr^G + b^G + J^G + I_1^G + \eta_{\rho_1}^G \quad (1)$$

$$\phi_1^G = r^G + dr^G + b^G + J^G - I_1^G + N_1^G + \eta_{\phi_1}^G \quad (2)$$

Where  $r$  is the true range,  $\rho$  is the pseudorange measurement,  $I$  is the ionospheric delay,  $J$  is the tropospheric delay,  $dr$  is the ephemeris error,  $b$  is the satellite clock error,  $\eta_{\rho}$  is the code-tracking noise and multipath,  $\phi$  is the carrier-phase measurement,  $N$  is the range ambiguity and  $\eta_{\phi}$  is the carrier-tracking noise and multipath.  $\blacksquare_1$  represents a variable for on the L1 signal,  $\blacksquare^G$  is used for parameters relating to the ground receivers and  $\blacksquare^A$  for those relating to the airborne receiver. Recalling the correction definitions and their associated models [8].

$$PRC_1 = r^G - \hat{\rho}_1^G = -dr^G - b^G - J^G - I_1^G - \epsilon_1^G \quad (4)$$

$$RRC_{1,k} = \frac{PRC_{1,k} - PRC_{1,k-1}}{T} = -d\hat{r}^G - \dot{b}^G - \dot{J}^G - \dot{I}_1^G - \dot{\epsilon}_1^G \quad (5)$$

Where  $\hat{\rho}_1^G$  is the smoothed pseudorange observable,  $I$  is the smoothed ionospheric delay,  $\epsilon$  represents smoothed

multipath and noise components and  $\dot{\phantom{x}}$  defines the linear derivative. The influence of the PRC-based receiver clock correction has been neglected in equations (4) and (5) as it introduces common mode-like errors which cancel in the airborne position solution. At the airborne receiver, the corrections are applied using the following expression:

$$\tilde{\rho}_1^A(t_A) = \hat{\rho}_1^A(t_A) + PRC_1 + t_{AZ}RRC_1 \quad (6)$$

Where  $t_{AZ}$  represents the time between the modified time of correction generation  $t_z$  and the time of application at the airborne receiver:  $t_{AZ} = t_A - t_z$ ,  $\hat{\rho}$  is the smoothed pseudorange measurement and  $\tilde{\rho}$  is the corrected pseudorange measurement. Equation (6) may be decomposed using equations (4) and (5) into the error components.

$$\begin{aligned} \tilde{\rho}_1^A(t_A) = & r^A + (dr^A - (dr^G + t_{AZ}d\dot{r}^G)) \quad (7) \\ & + (b^A - (b^G + t_{AZ}\dot{b}^G)) \\ & + (J^A - (J^G + t_{AZ}\dot{J}^G)) \\ & + (I_1^A - (I_1^G + t_{AZ}\dot{I}^G)) \\ & + (\epsilon_1^A - (\epsilon_1^G + t_{AZ}\dot{\epsilon}^G)) \end{aligned}$$

## IONOSPHERE-FREE SMOOTHING

Ionosphere-free (IF) smoothing may be used to eliminate the ionospheric delay term from the pseudorange observable and corrections. The inputs to the IF smoothing filter are defined as [7]:

$$\begin{aligned} \Phi_{IF}^G &= \phi_1^G - \frac{1}{\alpha}(\phi_1^G - \phi_5^G) \quad (8) \\ &= r^G + dr^G + b^G + J^G \\ &+ N_{\Phi 15} + \eta_{\Phi 15} \end{aligned}$$

$$\begin{aligned} \Psi_{IF}^G &= \rho_1^G - \frac{1}{\alpha}(\rho_1^G - \rho_5^G) \quad (9) \\ &= r^G + dr^G + b^G + J^G \\ &+ \eta_{\Psi 15} \end{aligned}$$

$$\begin{aligned} \text{With } \alpha &= 1 - \frac{f_1^2}{f_5^2}, \eta_{\Psi 15} = \eta_{\rho 1} - \frac{1}{\alpha}(\eta_{\rho 1} - \eta_{\rho 5}), \\ N_{\Phi 15} &= N_1 - \frac{1}{\alpha}(N_1 - N_5), \eta_{\Phi 15} = \eta_{\phi 1} - \frac{1}{\alpha}(\eta_{\phi 1} - \eta_{\phi 5}) \end{aligned}$$

The IF PRC and RRC may then be determined in a similar fashion to the GAST D SF case:

$$PRC_{IF} = r^G - \Phi_{IF}^G = -dr^G - b^G - J^G - \epsilon_{IF}^G \quad (10)$$

$$RRC_{IF} = \dot{PRC}_{IF} = \frac{(PRC_{IF,k} - PRC_{IF,k-1})}{T} \quad (11)$$

Where  $\epsilon_{IF}^G = F\eta_{\Psi_{IF}}^G + (1-F)\eta_{\Phi_{IF}}^G$  with  $F$  as the transfer function of the smoothing filter considered in the

Laplace domain or simply the filter operator in the time domain.

If we assume the same smoothing technique is applied to the airborne receiver, the corrected model is as follows:

$$\tilde{\Psi}_{IF}^A = \hat{\Psi}_{IF}^A + PRC_{IF} + t_{AZ}RRC_{IF} \quad (12)$$

$$\begin{aligned} \tilde{\Psi}_{IF}^A = & r^A + (dr^A - (dr^G + t_{AZ}d\dot{r}^G)) \quad (13) \\ & + (b^A - (b^G + t_{AZ}\dot{b}^G)) \\ & + (J^A - (J^G + t_{AZ}\dot{J}^G)) \\ & + (\epsilon_{IF}^A - (\epsilon_{IF}^G + t_{AZ}\dot{\epsilon}_{IF}^G)) \end{aligned}$$

## SINGLE FREQUENCY ERROR MODELS

### Ground Multipath and Noise

The residual error at the airborne receiver due to smoothed code multipath and noise can be described with the following equation:

$$\delta\epsilon = \epsilon_1^A - (\epsilon_1^G + t_{AZ}\dot{\epsilon}^G) \quad (14)$$

It is important to note that the term  $\dot{\epsilon}^G$  is the error contribution due to the change in the smoothed ground multipath and noise over the interval  $T$  at epoch  $k$ .

$$\dot{\epsilon}^G = \frac{\epsilon_{1,k}^G - \epsilon_{1,k-1}^G}{T} \quad (15)$$

Under the assumption of uncorrelated raw multipath and noise terms the residual error follows a zero-mean Gaussian distribution defined by:

$$\delta\epsilon \sim N(0, \sigma_\epsilon^2) \quad (16)$$

$$\sigma_\epsilon^2 = \sigma_{\epsilon^A}^2 + \sigma_{\epsilon^G}^2 + (t_{AZ})^2 \sigma_{\dot{\epsilon}^G}^2 \quad (17)$$

and  $\sigma_{\epsilon^A}$  is the standard deviation of the airborne multipath and noise,  $\sigma_{\epsilon^G}$ , the standard deviation of the multipath and noise on the pseudorange correction and  $\sigma_{\dot{\epsilon}^G}$  the standard deviation of the multipath and noise contribution to the RRC. The difference over two epochs in smoothed multipath and noise at the ground is then (see APPENDIX for derivation):

$$\epsilon_{1,k}^G - \epsilon_{1,k-1}^G \approx \eta_{1,\rho,k}^G \frac{T}{\tau} + \sqrt{2}\eta_{1,\phi,k}^G \quad (18)$$

where  $\eta_{1,\rho,k}^G$  is defined as the raw code multipath and noise component,  $\eta_{1,\phi,k}^G$  is defined as the phase multipath and noise component and  $\tau$  as the smoothing time constant, giving:

$$\dot{\epsilon}^G \approx \frac{\eta_{1,\rho,k}^G}{\tau} + \frac{\sqrt{2}}{T}\eta_{1,\phi,k}^G \quad (19)$$

The standard deviation of the contribution to the error rate in the smoothed multipath and noise can be expressed as:

$$\sigma_{\epsilon} \approx \sqrt{\left(\frac{\sigma_{\eta_{1,\rho}}^G}{\tau}\right)^2 + 2\left(\frac{\sigma_{\eta_{1,\phi}}^G}{T}\right)^2} \quad (20)$$

A conservative bound of 3mm is assumed for the phase noise element of  $\sigma_{\eta_{1,\phi}}^G$  (the impact of phase multipath is under review). Values of  $\sigma_{\eta_{1,\rho}}^G$  as a function of elevation have been obtained from the DLR experimental GBAS installation which is described in [12]. This elevation dependent model is likely conservative with respect to an operational station.

### Ionosphere + Troposphere

The single frequency differential residual error due to the ionospheric and tropospheric delays are expressed as follows:

$$\delta I = I_1^A - (I_1^G + t_{AZ}I_1^G) \quad (21)$$

$$\delta J = J^A - (J^G + t_{AZ}J^G) \quad (22)$$

In order to address the 2<sup>nd</sup>-order temporal effects of the nominal ionosphere and troposphere errors, they may be decomposed into spatial and temporal components.

$$\delta I = \underbrace{I_1^A(t_A) - I_1^G(t_A)}_{spatial} + \underbrace{I_1^G(t_A) - (I_1^G(t_G) + t_{AZ}I_1^G)}_{temporal} \quad (23)$$

$$\delta J = \underbrace{J^A(t_A) - J^G(t_A)}_{spatial} + \underbrace{J^G(t_A) - (J^G(t_G) + t_{AZ}J^G)}_{temporal} \quad (24)$$

Note that in nominal conditions when the smoothing filters within the ground and airborne subsystems are in steady states, the term  $I_1^G$  can be considered as a constant such that the temporal component will be zero and the residual differential ionospheric error will contain only a spatial component. It is currently under investigation within SESAR WP 15.3.7 as to whether  $J^G$  can be considered as a constant over the period of three smoothing windows. If so the residual differential error due to the troposphere will contain only a spatial component.

### Satellite Clock Error

The residual differential error due to Satellite Clock can be modelled with a zero-mean Gaussian [11]:

$$\delta b = b^A - (b^G + t_{AZ}\dot{b}^G) \quad (25)$$

$$\delta b \sim N(0, \sigma_b^2) \quad (26)$$

where  $\sigma_b$  is defined as it is described in details in [11] by the following expression:

$$\sigma_b^2 = \left(1 + \frac{t_{AZ}}{T}\right) t_{AZ} AVAR(1s) \quad (27)$$

with  $AVAR(1s)$  representing the Allan Variance at the order of 1s.

As it is explained in [11], the residual stochastic satellite clock time error after applying the PRC is a random walk resulting from the sum of independent Gaussian random variables. Since GBAS provides scalar corrections in the form of the PRC and RRC all the error types are combined. The RRC contains a term that corresponds to the satellite clock error rate, which in the mean will correspond to the deterministic component of the error that was not perfectly estimated by the constellation control segment and modelled by the broadcast clock correction clock error rate term. In [11], the effect of this linear prediction is analyzed. The conclusion is that it increases the residual satellite clock error by a factor  $\sqrt{\left(1 + \frac{t_{AZ}}{T}\right)}$  with respect to the error without applying the linear prediction correction.

By incorporating the impact of the RRC we obtained the following Figure 2 representing the residual satellite clock error as a function of  $t_{AZ}$  for the case where  $T = 0.5s$ .

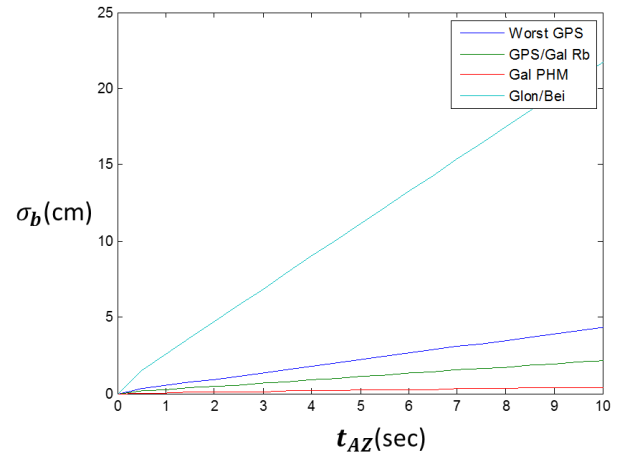


Figure 2 - Standard deviation of the Residual Satellite Clock Error over time

The standard deviation rises to a few centimeters for the worst performing GPS satellite over update periods up to 10s. Also, we note that with the improved expected performance for the Galileo clock over this time scale only a very small growth in the residual error standard deviation is seen. With regard to the clock errors, an extension of an update period (increasing of  $t_{AZ}$ ) to a few seconds appears feasible.

### Residual Ephemeris Error

The residual differential error due to Residual Ephemeris can be modelled by:

$$\delta dr = dr^A - (dr^G + t_{AZ}d\dot{r}^G) \quad (28)$$

As was the case for the environmental errors, we may split the error into spatial and temporal components:

$$\begin{aligned} \delta dr & \\ &= \underbrace{dr_1^A(t_A) - dr_1^G(t_A)}_{\text{spatial}} \\ &+ \underbrace{dr_1^G(t_A) - (dr_1^G(t_G) + t_{AZ} dr^G)}_{\text{temporal}} \end{aligned} \quad (29)$$

The RRC corrects for  $\dot{dr}^G$ , the temporal component is negligible and the mm level spatial error remains.

### Total Error

The RRC may be modelled at each epoch as containing a bias term relating to the true linear variation from ephemeris, satellite clock ionosphere and troposphere error rates as well as a stochastic term as a result of the code and phase multipath and noise, the stochastic satellite clock error and other random errors. The VDB data (e.g. Figure 3 and Figure 4) shows that the RRC bias is negligible with respect to its noise. Indeed, Figure 3 and Figure 4 depict the impact of elevation on RRC for both 30s and 100s smoothing constants.

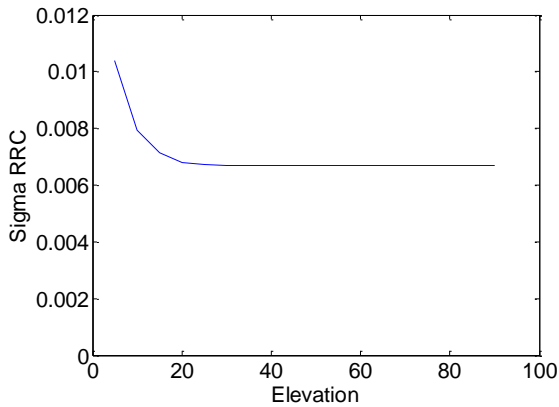


Figure 3 - Std for 100s smoothed RRC

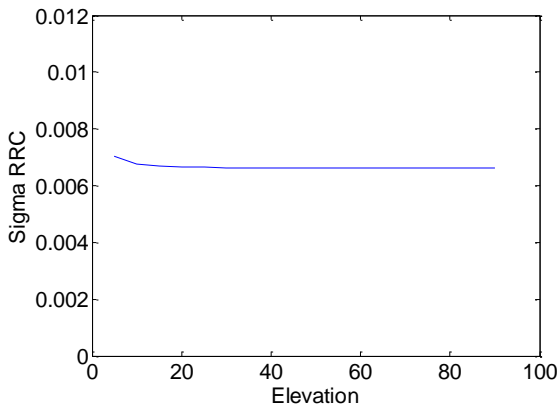


Figure 4 – Std for 30s smoothed RRC

Then, the total error model for  $\tilde{\rho}_1^A(t_A)$  can be expressed as follows:

$$\tilde{\rho}_1^A(t_A) \sim N(0, \sigma^2) \quad (30)$$

With

$$\begin{aligned} \sigma^2(\tau, T, t_{AZ}, el) & \\ &= \frac{(\sigma_\eta(el)T/(2\tau))^2 + (t_{AZ})^2 \left( (\sigma_{\eta_{i,p}}^G(el)/\tau)^2 + 2(\sigma_{\eta_{i,\phi}}^G/T)^2 \right)}{\text{gnd multipath + noise}} \\ &+ \frac{(1 + t_{AZ}/T)t_{AZ}AVAR(1s)}{\text{SV clock}} + \frac{\sigma_{\epsilon^A}^2(el)}{\text{air multipath + noise}} \\ &+ \frac{\sigma_{iono}(el)^2}{iono} + \frac{\sigma_{tropo}(el)^2}{tropo} \end{aligned} \quad (31)$$

Note that variations in smoothing filter type and time constant will impact  $\sigma_{\epsilon^A}$ ,  $\sigma_\eta$  &  $\sigma_{iono}$ . The impact of the correction update period extension has been derived. The standard deviation of the total error model for the corrected smoothed airborne pseudorange  $\tilde{\rho}_1^A(t_A)$  was determined for different processing options using the existing single-frequency smoothed observable and on the ionosphere-free (IF) and differing the smoothing constants. In this paper, only GPS L1 C/A and GPS L1/L5 IF are presented, though little dependency on constellation clock performance was found. Therefore, these results may be used for equivalent Galileo observables

Figure 5 shows the impact of elevation and  $t_{AZ}$  on the total standard deviation for GPS L1C/A and Figure 6 for the GPS L1-L5 IF case [7] with  $\tau = 100s$ . A GAD – C4 level is used for the ground code multipath component whilst an AAD B level is taken for the aircraft installation [8].

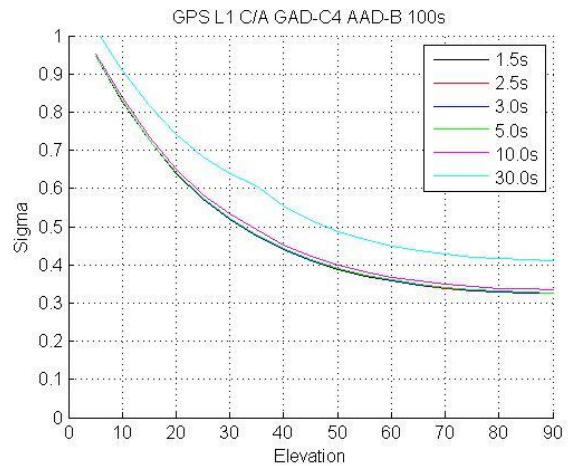


Figure 5 - Impact of elevation and  $t_{AZ}$  on the total standard deviation for GPS L1C/A with  $\tau = 100s$

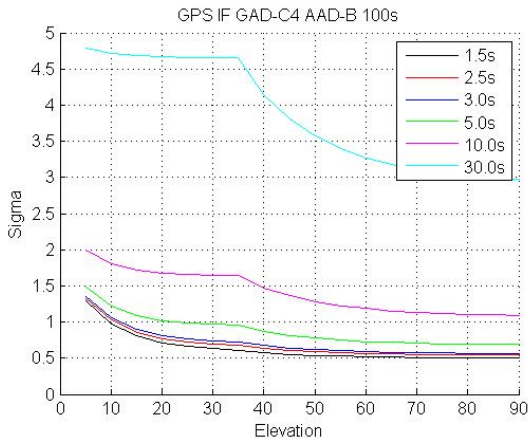


Figure 6 - Impact of elevation and  $t_{AZ}$  on the total standard deviation for GPS L1-L5 IF with  $\tau = 100s$

By comparing Figure 5 and Figure 6, the error budget seems inflated when using I-Free.

Figure 7 and Figure 8 represented below, show the difference in the standard deviation of the corrections for different extrapolation times of the GPS L1 C/A.

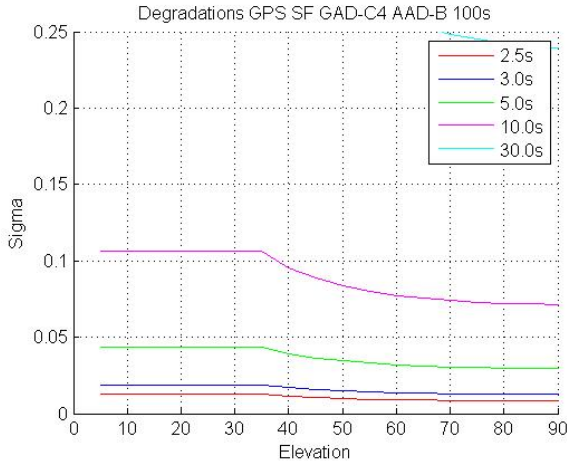


Figure 7 - 100s Smoothed Error Degradation with Update Period

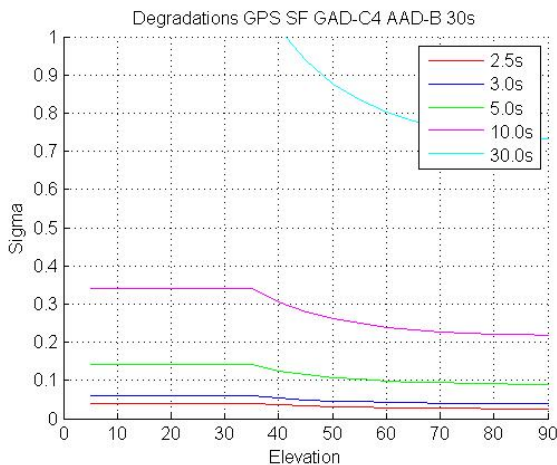


Figure 8 - 30s Smoothed Error Degradation with Update Period

The 30s standard deviation is higher than the 100s but in both cases, the highest value is of the order of 20cm for update periods up to 10s. There is only a minor difference of a couple of centimeters for update periods up to five seconds.

## DATA PROCESSING METHODOLOGY

According to the current GAST D requirements [10] based on the 2Hz correction rate,  $t_{AZ}$  must be inferior to 1.5s in the absence of lost VDB messages and airborne related delays. If the update period of the PRC is extended, this value will increase. There is then the need to examine the influence of higher  $t_{AZ}$ . In order to analyze the influence of an increased correction update period the current extrapolation of PRC of 1.5s was compared to longer extrapolation times  $t_{ex}$ . Figure 9 shows at the airborne receiver time  $t$  the difference between extrapolated PRC computed using PRC at  $t$ .

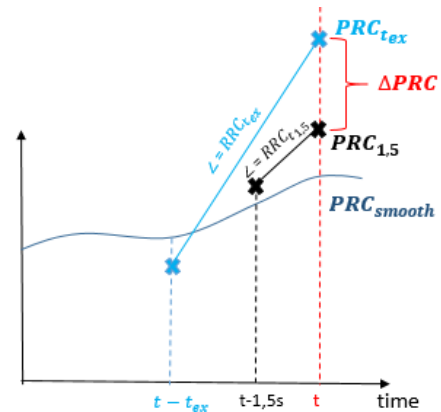


Figure 9– PRC and RRC over time

The following computation expresses the difference in the error using a longer extrapolation period to the current approach:

$$PRC_{t_{ex}}(t) = PRC(t - t_{ex}) + RRC(t - t_{ex}) \quad (32)$$

$$PRC_{1.5}(t) = PRC(t - 1.5) + RRC(t - 1.5) \quad (33)$$

$$\delta PRC_{1.5}(t) = |PRC_{1.5}(t) - PRC_{smooth}(t)| \quad (34)$$

$$\delta PRC_{t_{ex}}(t) = |PRC_{t_{ex}}(t) - PRC_{smooth}(t)| \quad (35)$$

$$\Delta PRC_{t_{ex}-1.5}(t) = \delta PRC_{t_{ex}}(t) - \delta PRC_{1.5}(t) \quad (36)$$

where  $PRC_{smooth}$  is the reference ‘true’ PRC obtained using a 20 point Gaussian filter. The set of positive  $\Delta PRC_{t_{ex}-1.5}$  is used to derive the statistics as this conservatively relates to the degradations in performance. The  $\Delta PRC$  will depend upon the statistical properties of the RRC which in turn may depend upon elevations. The standard deviations for the RRCs from MT1 and MT11 for  $5^\circ$  elevation bins are determined.

## DATA PROCESSING RESULTS

Three days of VDB message data obtained from the Thales GAST D prototype ground station installed at Toulouse Blagnac airport was processed. Figure 10 and Figure 11 represented below, show histograms of the RRC over all ranging sources for the MT1 and MT11 corrections.

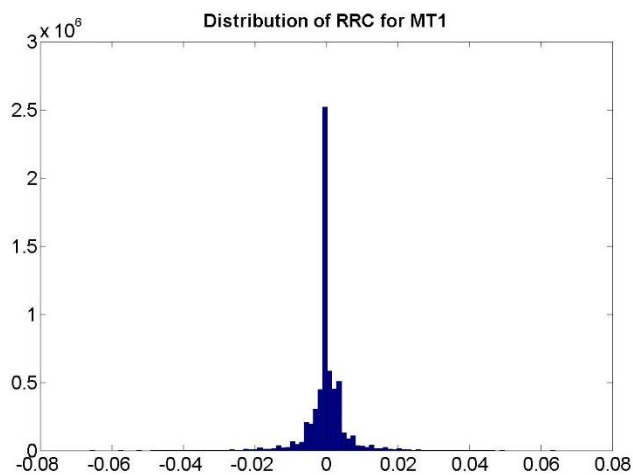


Figure 10 - Distribution of RRC for all satellites for MT1

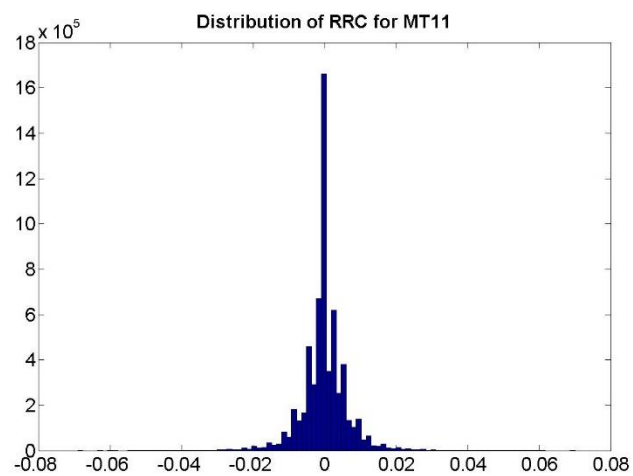


Figure 11- Distribution of RRC for all satellites for MT11

It is clear that these RRC distributions are central and in fact contain a high number of zero values (note that the resolution of the RRC is 1mm/s).

Then, a typical one minute interval of the RRC and its characteristic noise-like nature are visible in the following Figure 12.

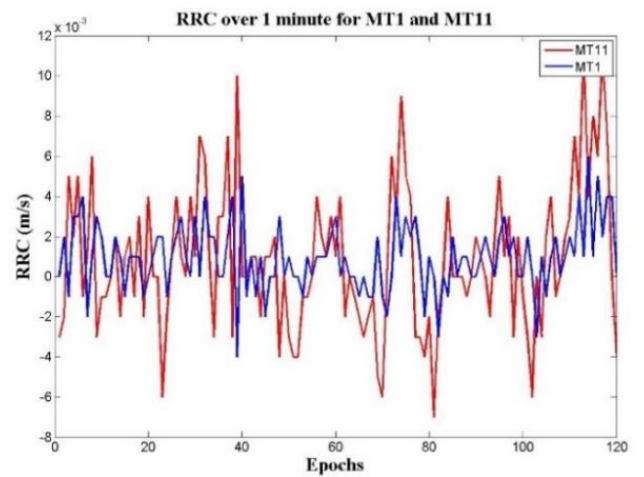


Figure 12 - RRC over 1minute

Standard deviations for RRCs from MT1 and MT11 were plotted as a function of elevation in Figure 13.

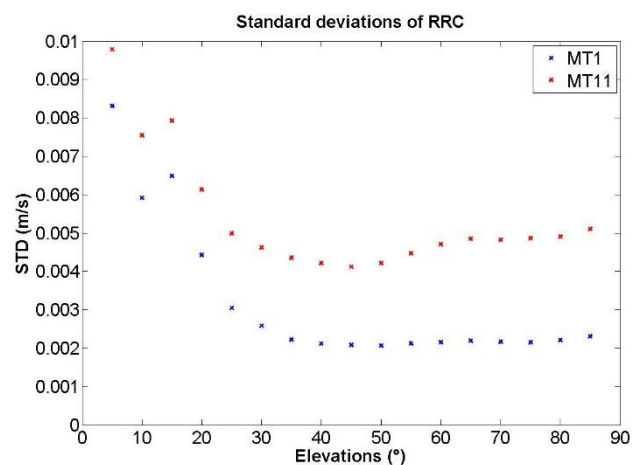


Figure 13- Standard deviation of RRC for MT1 (blue) and MT11 (red)

The standard deviation of RRC for MT1 takes values from 2-8mm/s and for MT11 takes values from 4-10mm/s. These intervals are similar but smaller than those found in theory (Figure 3 and Figure 4) where we have values from 7-10mm/s.

Finally, Figure 15 present the standard deviations of  $\Delta PRC$  for MT1 and MT11 for different update periods.

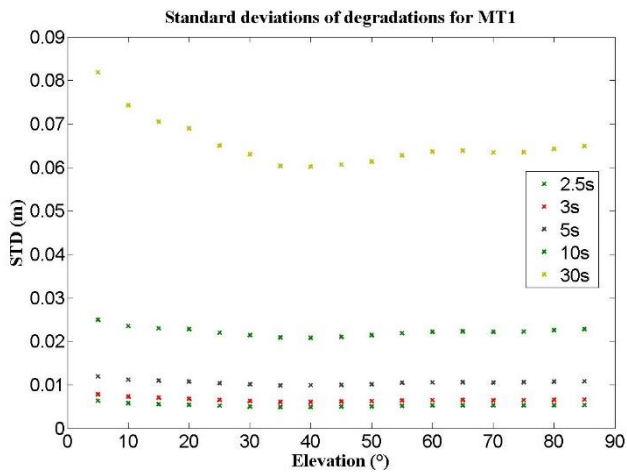


Figure 14 - Standard deviation of  $\Delta PRC$  for different time of extrapolation for MT1

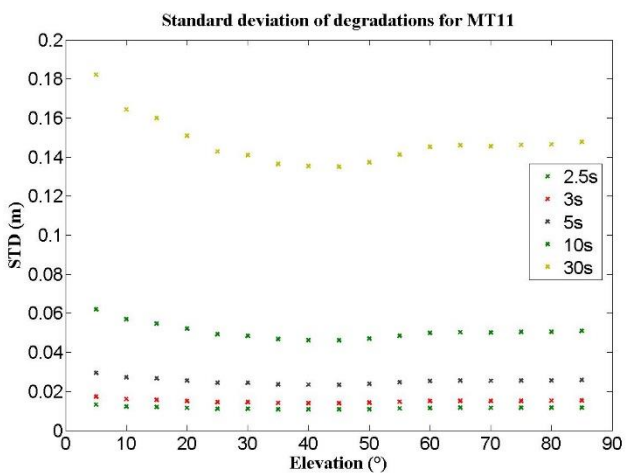


Figure 15 - Standard deviation of  $\Delta PRC$  for different time of extrapolation for MT11

The Figure 14 and Figure 15 show little dependency on elevation as was determined from the theoretical results and appears to confirm that the phase noise whose level only has a minor dependence on elevation is the primary contributor. However, the empirical results (Figure 12, Figure 13, Figure 14 and Figure 15) show a greater influence of the smoothing constant than as determined theoretically (Figure 7 and Figure 8). Indeed, the highest value for standard deviation is around 8cm for MT1 and 18cm for MT11 in the empirical curves and around 18 cm for MT1 and around 20cm for MT11 for the theoretical curves. This analysis suggests that the contribution of code multipath and noise is not sufficiently modelled in the theoretical derivation.

## SUMMARY

This paper has addressed the question of whether decreasing the frequency of correction messages in GBAS severely degrades the performance of the differential correction process under nominal, fault-free conditions. An

enhanced derivation of the differential satellite clock error has been presented and how the ground multipath and noise effects on both code and phase are inflated through the use of the RRC were analyzed.

The total error budget was derived to quantify the degradation as a function of the message update rate for the current MT1 and MT11 corrections based on 100s and 30s smoothing constants respectively. Theoretically, the standard deviations rise by a couple of centimeters over update periods up to 10s and thus an extension of the update period from nowadays 0.5s to say 3.5s appears feasible. As seen in the derivation of the IF smoothing, this effect will be inflated when using IF. The real data analysis found similar results to those derived theoretically and as expected due to conservative nature of the theoretical assumptions, the standard deviations of the resulting errors were smaller. The impact of smoothing between the two approaches requires further work.

## ACKNOWLEDGMENTS

The authors would like to thank the DSN and Thales Electronic Systems for the provision of data from the prototype GAST D ground station and partners of the SESAR WP 15.3.7. They would also like to thank Frieder Beck for his advice regarding the ground subsystem extrapolation computations.

“©SESAR JOINT UNDERTAKING, 2013. Created by ENAC, DSN and Thales Electronic Systems for the SESAR Joint Undertaking within the frame of the SESAR Programme co-financed by the EU and EUROCONTROL. The opinions expressed herein reflect the author's view only. The SESAR Joint Undertaking is not liable for the use of any of the information included herein. Reprint with approval of publisher and with reference to source code only.”

## REFERENCES

- [1] ICAO, Annex 10 to the Convention on the International Civil Aviation Volume I (Radio Navigation Aids), 5th Edition, Amendment 83, 2007.
- [2] J. Burns, ICAO NSP - Conceptual Framework for the proposal for the Proposal for GBAS to Support CAT III Operations, draft version 6.5, ICAO NSP WG, November 2009.
- [3] SESAR JU, D03, SESAR 15.3.6 - High Performance Allocation and Split of Responsibilities between Air and Ground.
- [4] M. Stakkeland, Y. L. Andalsvik et S. Knut, «Estimating Satellite Excessive Acceleration in the Presence of Phase Scintillations,» chez ION GNSS 2014, 2014.

- [5] F. Beck, O. Glaser et B. Vauvy, «Standards – Draft Standards for Retained Galileo GBAS Configurations».
- [6] T. Walter, J. Blanch and P. Enge, “Implementation of the L5 SBAS MOPS,” in *ION GNSS 2013*, 2013.
- [7] P. Y. M. G. A. & B. J. R. HWANG, «Enhanced DifferentialGPS Carrier-Smoothed Code Processing Using Dual-Frequency Measurements,» *Journal of The Institute of Navigation*, vol. 46, n° 12, 1999.
- [8] RTCA Inc., Minimum Operational Performance Standards (MOPS) for GPS Local Area Augmentation System (LAAS) Airborne Equipment - RTCA DO-253C, Washington DC, 2008.
- [9] RTCA Inc., MASPS for LAAS - RTCA DO-245A, Washington DC, 2004.
- [10] RTCA.Inc, RTCA DO-246D - GNSS-Based Precision Approach Local Area Augmentation System (LAAS) Signal-in-Space Interface Control Document (ICD), 2008.
- [11] SESAR(JU), «Satellite constellations and Signals - Int ST3.3-WP15.03.07 Multi GNASS CAT II/III GBAS,» 2014.
- [12] M.-S. Circiu, M. Felux, P. Remi, L. Yi, B. Belabbas et S. Pullen, «Evaluation of Dual Frequency GBAS Performance using flight Data,» *ITM 2014*.

## APPENDIX

In this appendix the following approximate relation is derived:

$$\begin{aligned} \epsilon_{1,k}^G - \epsilon_{1,k-1}^G &\approx \eta_{1,\rho,k}^G \frac{T}{\tau} + \sqrt{2} \eta_{1,\phi,k}^G \\ \hat{\rho}_k &= \left(1 - \frac{T}{\tau}\right)^k (\rho_0 - \phi_0) + \frac{T}{\tau} \left[ \sum_{n=1}^k \left(1 - \frac{T}{\tau}\right)^{k-n} (\rho_n - \phi_n) \right] \\ &\quad + \phi_k \\ \hat{\rho}_k &= \left(1 - \frac{T}{\tau}\right)^k (\rho_0 - \phi_0) + \frac{T}{\tau} \left[ \sum_{n=1}^{k-2} \left(1 - \frac{T}{\tau}\right)^{k-n} (\rho_n - \phi_n) \right] \\ &\quad + \left(\frac{T}{\tau}\right) \left(1 - \frac{T}{\tau}\right) \rho_{k-1} - \left(\frac{T}{\tau}\right) \left(1 - \frac{T}{\tau}\right) \phi_{k-1} \\ &\quad + \left(\frac{T}{\tau}\right) \rho_k + \left(1 - \frac{T}{\tau}\right) \phi_k \\ \hat{\rho}_{k-1} &= \left(1 - \frac{T}{\tau}\right)^{k-1} (\rho_0 - \phi_0) \\ &\quad + \frac{T}{\tau} \left[ \sum_{n=1}^{k-1} \left(1 - \frac{T}{\tau}\right)^{k-1-n} (\rho_n - \phi_n) \right] + \phi_{k-1} \end{aligned}$$

$$\begin{aligned} \hat{\rho}_{k-1} &= \left(1 - \frac{T}{\tau}\right)^{k-1} (\rho_0 - \phi_0) \\ &\quad + \frac{T}{\tau} \left[ \sum_{n=1}^{k-2} \left(1 - \frac{T}{\tau}\right)^{k-1-n} (\rho_n - \phi_n) \right] \\ &\quad + \left(\frac{T}{\tau}\right) \rho_{k-1} + \left(1 - \frac{T}{\tau}\right) \phi_{k-1} \end{aligned}$$

$$\begin{aligned} \text{We have } &\left(1 - \frac{T}{\tau}\right)^k (\rho_0 - \phi_0) - \left(1 - \frac{T}{\tau}\right)^{k-1} (\rho_0 - \phi_0) \\ &= \left(-\frac{T}{\tau}\right) \left(1 - \frac{T}{\tau}\right)^{k-1} (\rho_0 - \phi_0) \end{aligned}$$

Then when  $k$  has a high value, we can assume that this difference is negligible by the fact that  $\tau$  is much higher than  $T$ .

So, we approximate the difference:

$$\begin{aligned} \hat{\rho}_k - \hat{\rho}_{k-1} &\approx \frac{T}{\tau} \left[ \sum_{n=1}^{k-2} \left( \left(1 - \frac{T}{\tau}\right)^{k-n} - \left(1 - \frac{T}{\tau}\right)^{k-1-n} \right) (\rho_n - \phi_n) \right] \\ &\quad - \left(\frac{T}{\tau}\right)^2 \rho_{k-1} + \left(\left(\frac{T}{\tau}\right)^2 - 1\right) \phi_{k-1} \\ &\quad + \left(\frac{T}{\tau}\right) \rho_k + \left(1 - \frac{T}{\tau}\right) \phi_k \end{aligned}$$

$$\begin{aligned} \hat{\rho}_k - \hat{\rho}_{k-1} &\approx -\left(\frac{T}{\tau}\right)^2 \left[ \sum_{n=1}^{k-2} \left(1 - \frac{T}{\tau}\right)^{k-1-n} (\rho_n - \phi_n) \right] \\ &\quad - \left(\frac{T}{\tau}\right)^2 \rho_{k-1} + \left(\left(\frac{T}{\tau}\right)^2 - 1\right) \phi_{k-1} + \left(\frac{T}{\tau}\right) \rho_k \\ &\quad + \left(1 - \frac{T}{\tau}\right) \phi_k \end{aligned}$$

$$\begin{aligned} \hat{\rho}_k - \hat{\rho}_{k-1} &\approx -\left(\frac{T}{\tau}\right)^2 \left[ \sum_{n=1}^{k-2} \left(1 - \frac{T}{\tau}\right)^{k-1-n} (\rho_n - \phi_n) \right] \\ &\quad - \left(\frac{T}{\tau}\right)^2 \rho_{k-1} + \left(\left(\frac{T}{\tau}\right)^2 - 1\right) \phi_{k-1} + \left(\frac{T}{\tau}\right) \rho_k \\ &\quad + \left(1 - \frac{T}{\tau}\right) \phi_k \end{aligned}$$

$$RRC = \frac{-\hat{\rho}_k + \hat{\rho}_{k-1}}{T}$$

$$\begin{aligned} \sigma_{RRC}^2 &\approx \frac{T^2}{\tau^4} \left[ \sum_{n=1}^{k-2} \left(1 - \frac{T}{\tau}\right)^{2k-2-2n} \right] (\sigma_\rho^2 + \sigma_\phi^2) + \frac{T^2}{\tau^4} \sigma_\rho^2 \\ &\quad + \left(\frac{1 - \left(\frac{T}{\tau}\right)^2}{T}\right)^2 \sigma_\phi^2 + \frac{1}{\tau^2} \sigma_\rho^2 + \frac{\left(1 - \frac{T}{\tau}\right)^2}{T^2} \sigma_\phi^2 \end{aligned}$$

$$\begin{aligned} \sigma_{RRC}^2 &\approx \frac{T^2}{\tau^4} \left[ \frac{1 - \left(1 - \frac{T}{\tau}\right)^{2k-4}}{1 - \left(1 - \frac{T}{\tau}\right)^2} \right] (\sigma_\rho^2 + \sigma_\phi^2) + \frac{T^2}{\tau^4} \sigma_\rho^2 \\ &\quad + \left(\frac{1 - \left(\frac{T}{\tau}\right)^2}{T}\right)^2 \sigma_\phi^2 + \frac{1}{\tau^2} \sigma_\rho^2 + \frac{\left(1 - \frac{T}{\tau}\right)^2}{T^2} \sigma_\phi^2 \end{aligned}$$

$$\sigma_{RRC}^2 \approx \frac{T^2}{\tau^4} \left[ \frac{\tau}{2T} \right] (\sigma_\rho^2 + \sigma_\phi^2) + \frac{T^2}{\tau^4} \sigma_\rho^2 + \frac{1}{\tau^2} \sigma_\rho^2 + \frac{2}{T^2} \sigma_\phi^2$$

$$\sigma_{RRC}^2 \approx \frac{1}{\tau^2} \sigma_\rho^2 + \frac{2}{T^2} \sigma_\phi^2$$

Given that we're considering code and phase multipath assumed to be zero mean, this expression for the RRC variance is equivalent to:

$$\epsilon_{1,k}^G - \epsilon_{1,k-1}^G \approx \eta_{1,\rho,k}^G \frac{T}{\tau} + \sqrt{2} \eta_{1,\phi,k}^G$$